

# Effect of Fatty Acids on the Strain-Induced Crystallization of Natural Rubber Detected by Tear Energy Measurements

Tetsuji Kawazura,<sup>1</sup> Seiichi Kawahara,<sup>2</sup> Yoshinobu Isono<sup>2</sup>

<sup>1</sup>R & D Center, Yokohama Rubber Company, Limited, 2-1, Oiwake, Hiratsuka Kanagawa 254-8601, Japan

<sup>2</sup>Department of Chemistry, Faculty of Engineering, Nagaoka University of Technology, Nagaoka, Niigata 940-2188, Japan

Received 24 August 2003; accepted 13 January 2005

DOI 10.1002/app.22066

Published online in Wiley InterScience (www.interscience.wiley.com).

**ABSTRACT:** The strain-induced crystallization of natural rubber (NR) was investigated by the measurement of the tear energy of a crosslinked blend consisting of NR and noncrystalline styrene–butadiene rubber (SBR). When NR was dispersed into the SBR matrix, the tear energy of SBR increased at various temperatures and tear rates. After the application of the principle of time–temperature superposition to the tear energy according to the Williams–Landel–Ferry equation, two distinct curves were found for the NR/SBR blend with respect to the reduced tear rate, despite the fact that the tear energy of SBR or the SBR/SBR blend gave its own single composite curve. When the fatty acid in the

NR/SBR blend was removed by acetone extraction, the tear energy of the blend drew a single composite curve. The conversion of the two curves into the single composite curve for the NR/SBR blend suggested that the tear energy depended on the strain-induced crystallization of NR dispersed in the SBR matrix, which was suppressed by the removal of the fatty acid. © 2005 Wiley Periodicals, Inc. *J Appl Polym Sci* 98: 613–619, 2005

**Key words:** blends; crystallization; mechanical properties; rheology; rubber

## INTRODUCTION

Rapid strain-induced crystallization has been associated with the outstanding mechanical properties characteristic of crosslinked natural rubber (NR) in comparison with those of a synthetic analogue, that is, crosslinked *cis*-1,4-polyisoprene.<sup>1</sup> This may be due in part to a reinforcing effect of strain-induced crystals on the properties of NR as a filler or physical crosslinking point. In fact, the tensile and tear strengths of crosslinked NR are practically higher than those of crosslinked synthetic *cis*-1,4-polyisoprene at a high speed limit of the tear test.<sup>1</sup> However, factors influencing the rapid strain-induced crystallization have still remained ambiguous because of the difficulty of detecting the rapid crystallization reproducibly. It is thus quite important to suppress the crystallization without disturbing the long sequence of *cis*-1,4-isoprene units.

In a previous study,<sup>2</sup> we reported that the rate of crystallization of NR could be controlled by the dispersion of NR into styrene–butadiene rubber (SBR), in which rapid crystallization due to heterogeneous nucleation occurred when the average diameter of the

droplet was longer than about 1  $\mu\text{m}$ . Furthermore, the rate of crystallization was confirmed to depend on not only the diameter but also the dimension of the NR phase.<sup>3</sup> Because the isothermal crystallization of NR was promoted by a fatty acid, which was inherently present in NR and acted as a nucleating agent,<sup>4,5</sup> it may be possible to relate the rate of crystallization with the distribution of the fatty acid among the NR domains. Thus, the outstanding mechanical properties and rapid strain-induced crystallization of NR may be represented as a function of the number of nuclei, that is, the fatty acid, with respect to the diameter and dimensions of the NR domains.

To investigate both the outstanding mechanical properties and rapid strain-induced crystallization of NR, we take notice of the tear energy ( $G$ ) of the NR/SBR blend because the strain-induced crystallization of NR must play an important role in preventing crack growth of the blend under large deformation.  $G$  of a noncrystalline polymer is well known to depend on the rate of tear and the temperature, and a principle of time–temperature superposition according to the Williams–Landel–Ferry (WLF) equation<sup>6</sup> can be applied to it.  $G$  increases when a filler such as carbon black or silica is loaded into the polymer without a significant change in the shift factor ( $a_T$ ). Thus, the strain-induced crystallization of NR may be assessed by the measurement of  $G$  of a noncrystalline polymer containing an NR dispersoid because of the reinforcing effect of the

Correspondence to: T. Kawazura (t-kwzr@mta.yrc.co.jp).  
Contract grant sponsor: Yokohama Rubber Co., Ltd.

dispersoid, that is, strain-induced crystals as fillers. Furthermore, it is expected that a variation of the reinforcing effect depending on the temperature and rate of tear will be detected because the strain-induced crystallization of the dispersoid is a function of the parameters.

In this study, a model immiscible polymer blend, that is, a crosslinked NR/SBR blend, was used for the measurement of  $G$ . To estimate the crosslink densities of the NR phase and SBR phase in the NR/SBR blend, a differential swelling method proposed for immiscible polymer blends<sup>7</sup> was applied with good and poor solvents. The principle of time-temperature superposition was applied to measure  $G$  of the blend and that of the corresponding SBR over wide ranges of temperatures and tear rates, and the resultant composite curves were compared to demonstrate the contribution of the NR dispersoid and the stress-induced crystallization of the dispersoid. Furthermore, an effect of the fatty acid on the strain-induced crystallization of NR was investigated.

## EXPERIMENTAL

NR used in this study was SMR-L (standard Malaysian rubber). Nipol 1502 (styrene concentration = 23.5 wt %, vinyl concentration in polybutadiene = 15.1 mol %) and Nipol NS-116R (styrene concentration = 21 wt %, vinyl concentration in polybutadiene = 67.0 mol %), both supplied by Nippon Zeon Co., Ltd. (Kawasaki, Japan), were used as SBR1 and SBR2, respectively.

NR was masticated on a roll mill (150 mm × 380 mm, gap = 0.1 mm) for 5 min before use. Blend samples NR/SBR1 and SBR2/SBR1 (30/70 w/w) were also prepared by the mixing of SBR1 and SBR2, respectively, with masticated NR on the roll mill. Reagent-grade dicumyl peroxide (DCP) was added to NR, SBR1, and the blends, and then they were cured on a hot press at 15 MPa and 444 K for 10 min.

The crosslink density of NR and SBR1 was determined in terms of the Flory-Rehner expression<sup>8</sup> by the swelling of the rubber in benzene in the dark for a week. The crosslink density of each phase that appeared in the binary mixtures, that is, NR/SBR1 and SBR2/SBR1, was estimated from the swelling ratio in both benzene and *n*-heptane by the differential swelling method.<sup>7</sup> The values of an interaction parameter ( $\chi$ ) between the polymer and the solvent for NR and SBR1 in the literature<sup>9,10</sup> were used. An unknown value of  $\chi$  for SBR2 was estimated from a series of swelling measurements in benzene and *n*-heptane for specimens with different crosslink densities controlled by the DCP feed between  $7.10 \times 10^{-6}$  and  $2.72 \times 10^{-5}$  mol/mL. Equation (1) was applied to each crosslinked specimen:

$$\nu \equiv \frac{S_B + \chi_B S_B^2 + \ln(1 - S_B)}{V_B(S_B^{1/3} - S_B/2)} = \frac{S_H + \chi_H S_H^2 + \ln(1 - S_H)}{V_H(S_H^{1/3} - S_H/2)} \quad (1)$$

where  $\nu$ ,  $s$ , and  $V$  are the crosslink density of the polymer, the volume fraction of the polymer in the swelling specimen, and the molar volume of the solvent, respectively; the subscripts are used to designate the different solvents. Equation (1) can be rewritten as eq. (2), and  $\chi_B$  and  $\chi_H$  are obtained as the intercept and slope of a plot of  $Y$  versus  $X$ . The estimated  $\chi$  values of SBR2 at 298 K were 0.524 for benzene and 0.645 for *n*-heptane:

$$Y = \chi_B + \chi_H X \quad (2)$$

where

$$X = \frac{-V_B(S_B^{1/3} - S_B/2)S_H^2}{V_H S_B^2(S_H^{1/3} - S_H/2)},$$

$$Y = \frac{V_B(S_B^{1/3} - S_B/2)[S_H + \ln(1 - S_H)]}{V_H S_B^2(S_H^{1/3} - S_H/2)} - \frac{1}{S_B^2}[S_B + \ln(1 - S_B)]$$

Acetone extraction of the specimens of the blend and NR was performed in the dark under a nitrogen atmosphere with a Soxhlet apparatus for 72 h, and this was followed by drying under reduced pressure at room temperature for 5 days. The infrared spectrum was measured with a PerkinElmer (Boston, MA) System 2000 Fourier transform infrared (FTIR) instrument equipped with an attenuated total reflection attachment to confirm the removal of the free fatty acid by the acetone extraction. Each specimen for FTIR was taken from the strip with a clean knife, and a measurement was taken for a fresh section of the specimen.

The observation of the morphology of the blends was performed with a Hitachi (Tokyo, Japan) H-800 transmission electron microscope at an accelerating voltage of 100 kV. The ultrathin sections of the blends were prepared with an ultramicrotome equipped with a Leica (Vertrieb, Germany) Ultra Cut UCT cryo kit at a temperature lower than the glass-transition temperature of the samples. The sections were stained with RuO<sub>4</sub> for the NR/SBR1 blend and with OsO<sub>4</sub> for the SBR2/SBR1 blend.

Time-temperature shift factors ( $a_T$ ) for NR, SBR1, and SBR2 were estimated from data of the viscoelastic properties, which were measured with a dynamic mechanical analyzer (DVE-4A, UBM Co., Ltd., Kyoto, Japan) from 253 to 333 K and from 10 to 300 Hz.

The measurement of the tear strength was carried out with trouser-type strips, as shown in Figure 1(a), at various temperatures and cutting speeds. Here the

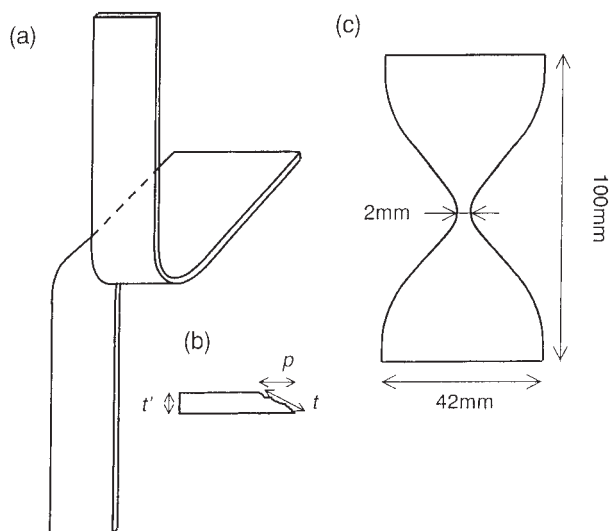


**Figure 1** Schematic drawings of samples for the measurements of (a) the tear strength and (c) the tensile strength and (b) a typical cross section of the torn strip.  $t$  was estimated from  $p$  and  $t'$ .

cutting speed was defined as a mean value for the crosshead speed of the testing machine because this was identical to that of the cutting speed.  $G$  was calculated as follows:

$$G = 2F/t \quad (3)$$

where  $F$  is the tear force and  $t$  is the width of the torn path. The average value of the tear strength along the torn path was used as  $F$ . Because the surface generated by tearing was not often accurately perpendicular to the surface of the strip,  $t$  was not identical to the thickness of the strip ( $t'$ ) and varied along the path. To estimate an accurate value of  $t$ , the average value of the projected width ( $p$ ) along the torn path was obtained by image analysis. NIH Image, which is an image processing and analysis program developed by the National Institutes of Health, with a specially designed macro program was used to obtain the average value of  $p$  from digital images of the torn stripes. Consequently,  $t$  was estimated from  $p$  and  $t'$  [see the schematic drawing in Fig. 1(b)].

The tensile strength was measured at a fixed stretching rate, that is, 5 mm/min, with specially designed specimens [Fig. 1(c)] to lead to rupture at a specific point. The temperature in the chamber used for the measurements of the tear strength and the tensile strength was controlled within  $\pm 0.1$  K during all the measurements.

## RESULTS AND DISCUSSION

The crosslink densities of the samples used in this study are tabulated in Table I. The crosslink density

for SBR1 was  $1.85 \times 10^{-4}$  mol/mL, which was similar to that for the SBR1 phase in the NR/SBR1 and SBR2/SBR1 blends. On the other hand, the crosslink density for NR was identical to that for the NR phase in the NR/SBR1 blend. This may allow us to investigate the reinforcing effect by the stress-induced crystalline dispersoid, that is, NR, on  $G$  of SBR because the crystallization of NR is known to be dependent on both the crosslink density<sup>11</sup> and the size of the dispersoid.<sup>3</sup>

Figure 2(a,b) shows transmission electron microscopy (TEM) photographs for the NR/SBR1 and SBR2/SBR1 blends, respectively; the dark phase is assigned to SBR1. For the NR/SBR1 blend, NR was found to be a domain, the particle diameter of which ranged from 1 to 2  $\mu\text{m}$ . In contrast, for the SBR2/SBR1 blend, SBR2 was dispersed in SBR1 as a fine ellipsoid of about 0.5  $\mu\text{m}$  in major ellipse. Thus, SBR1 was confirmed to be a matrix in the blends, whereas NR and SBR2 were domains.

To investigate the effect of the strain-induced crystallization of NR on  $G$  of SBR,  $G$  of NR/SBR1 was compared with that of SBR1.  $G$  for NR/SBR1 measured at various cutting speeds ( $R$ ), that is, 0.5, 5.0, 50, 500, and 1000 mm/min, is shown in Figure 3.  $G$  increased gradually as  $R$  increased. At the definite  $R$ ,  $G$  depended on the temperature and increased abruptly at 273 K. In contrast, a monotonic increase in  $G$  of SBR1 is shown against both  $R$  and the temperature in Figure 4. The absolute value of  $G$  for SBR1 was lower than that for NR/SBR1. According to a previous report by Stager et al.,<sup>12</sup> the difference in  $G$  between SBR1 and NR/SBR1 may be attributed to the effect of the strain-induced crystallization of NR.

Because  $G$  of a noncrystalline polymer is associated with a viscoelastic energy dissipation brought on by the deformation of the polymer, it can be analyzed in terms of the WLF rate-temperature equivalence.<sup>13,14</sup> To investigate the reinforcing effect of NR on SBR1, in this study, the rate-temperature equivalence was applied to  $G$  of SBR1 and NR/SBR1 under the assumption that the energy dissipation was independent of the crystalline domain, as in the case of the reinforcing effect of a filler such as carbon black or silica.<sup>6,15</sup> Figure 5 shows a master curve of  $\tan \delta$  for SBR1, which was obtained by the plotting of  $\tan \delta$  versus the reduced

**TABLE I**  
Crosslink Density ( $\nu$ ; mol/mL  $\times 10^{-4}$ ) of the Samples  
Estimated from Equilibrium Swelling

Sample	$\nu$		
	NR phase	SBR1 phase	SBR2 phase
NR/SBR1 (3/7)	0.742	2.10	
NR	0.842		
SBR1		1.85	
SBR2/SBR1 (3/7)		1.48	53.0

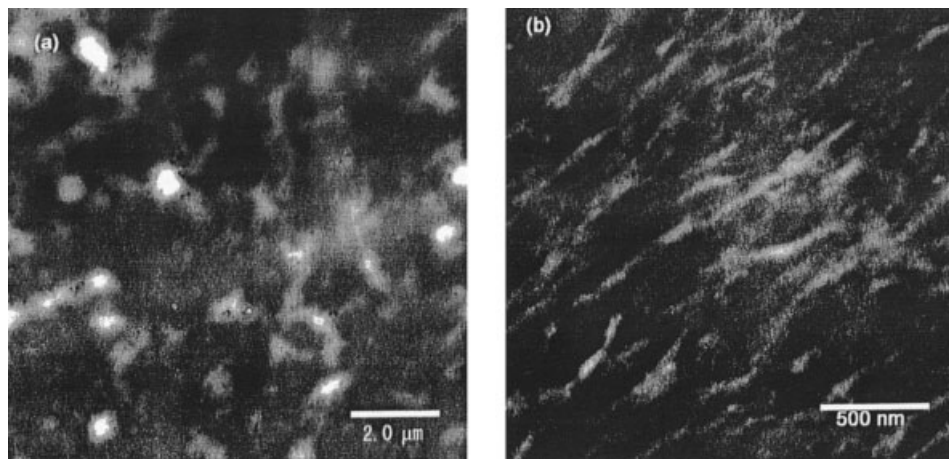


Figure 2 TEM photographs of (a) the NR/SBR1 blend and (b) the SBR2/SBR1 blend.

frequency with an angular frequency ( $\omega$ ) and a rate-temperature shift factor ( $a_T$ ):

$$\log a_T = -8.86(T - T_s)/(101.6 + T - T_s) \quad (4)$$

where  $T$  is temperature and the reference temperature ( $T_s$ ) is 268 K.  $a_T$  was also applied to  $\tan \delta$  for NR and SBR2 to draw the master curves ( $T_s = 251$  and 293 K, respectively).

The resultant curves after the superposition of  $G$  for NR/SBR1 and SBR1 are shown in Figure 6 ( $T_s = 268$  K). The principle of time-temperature superposition was completely applied for  $G$  of SBR1, as reported by Greensmith and Thomas.<sup>16</sup> This suggests that the change in  $G$  was associated with an energy dissipation of SBR1. In contrast,  $G$  for NR/SBR1 was divided into two curves after superposition: one for  $G$  measured at 273 K and the other at temperatures ranging from 298 to 333 K. This may be due to either an unsuitable  $a_T$  value used for the superposition of  $G$  or the strain-

induced crystallization of NR. Thus, the superposition of  $G$  was investigated with various  $a_T$  values, with a correlation coefficient ( $r$ ) estimated at a given  $T_s$  between 251 and 268 K, where  $r$  represents a scatter of data points from a regression curve. Figure 7 shows plots of the estimated  $r$  values versus  $T_s$  for the NR/SBR1 blend: one for  $G$  measured at 273 K and the other for  $G$  measured at 298, 313, and 333 K. The values of  $r$  for  $G$  measured at 298, 313, and 333 K depended on  $T_s$ , whereas that measured at 273 K did not. The former increased as  $T_s$  rose, and this implied a good superposition of  $G$ ; it reached its highest point at 265 K, and this reflected the dominant effect of the SBR1 matrix on the energy dissipation of the blend. This suggests that the two curves after the superposition of  $G$  for the NR/SBR1 blend may be due to the effect of the strain-induced crystallization of the NR domain. Consequently, the crystalline part of NR may increase  $G$ .

To ensure the effect of the strain-induced crystallization on  $G$  for the NR/SBR1 blend, the tensile strength of NR was measured at various temperatures

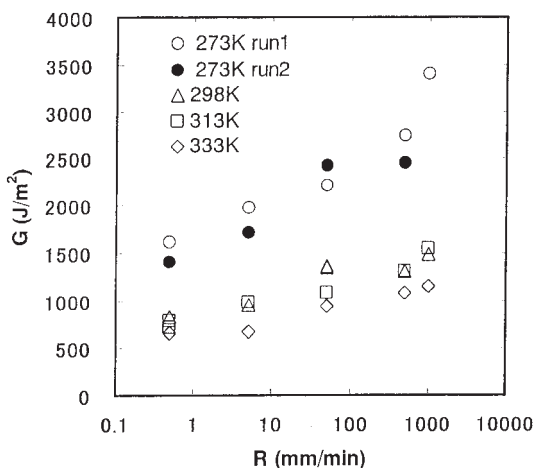


Figure 3 Temperature and  $R$  dependence of  $G$  for the NR/SBR1 blend.

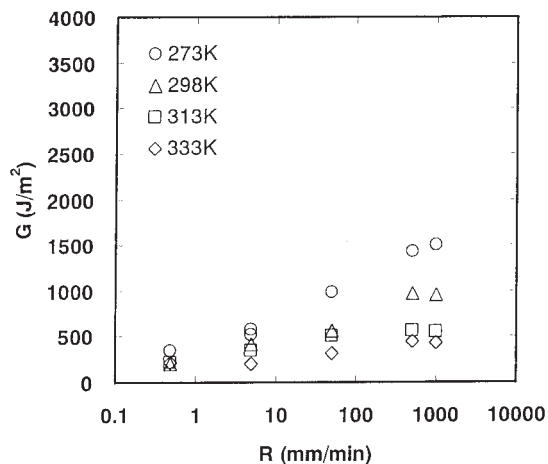


Figure 4 Temperature and  $R$  dependence of  $G$  for SBR1.

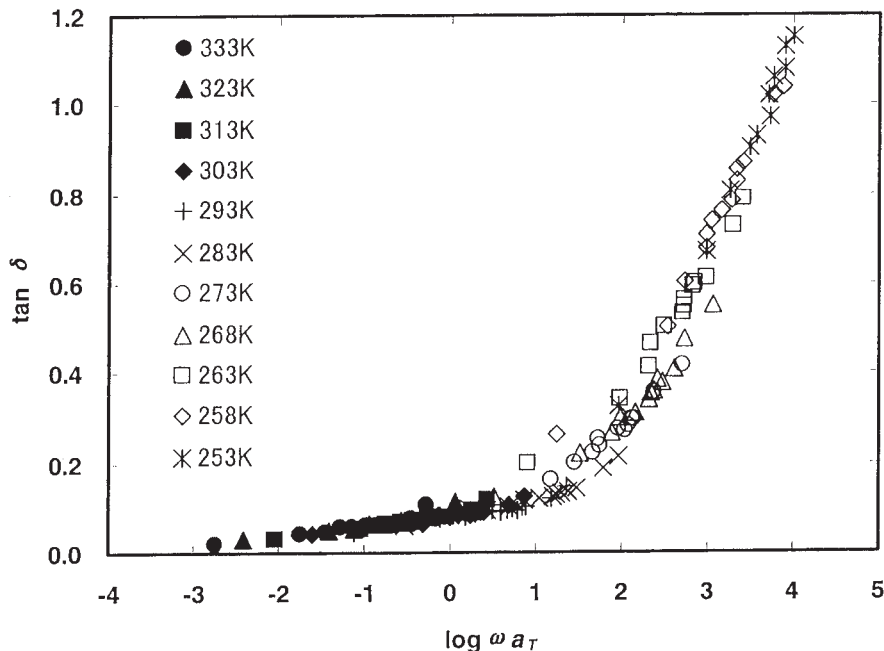


Figure 5 Plot of  $\tan \delta$  for SBR1 as a function of  $\log \omega a_T$  [ $a_T = -8.86(T - T_s)/(101.6 - T - T_s)$ ,  $T_s = 268$  K].

because it is well known to fall at the melting temperature of the strain-induced crystal.<sup>1,11</sup> Figure 8 shows the temperature dependence of the tensile strength of NR, the crosslink density of which was the same as that of NR in the NR/SBR1 blend. The tensile strength fell at about 293 K, at which melting of the strain-induced crystal of NR occurred. This may be supporting evidence that the abrupt drop in  $G$  for the NR/SBR1 blend was due to melting of the strain-induced crystal at about 293 K.

Instead of dispersed NR, the effect of noncrystalline SBR2 on  $G$  for SBR1 was investigated. Figure 9 shows a logarithmic plot of  $G$  versus the reduced cutting speed ( $Ra_T$ ) for the SBR2/SBR1 blend;  $G$  for the SBR2/SBR1 blend gives a single curve with  $a_T$  of SBR1, in contrast to the case of the NR/SBR1 blend. The logarithm of  $G$  for the SBR2/SBR1 blend was a function of the logarithm of  $Ra_T$ , and  $G$  for the SBR2/SBR1 blend was almost identical to that for SBR1; this implied little reinforcing effect of SBR2. These are distin-

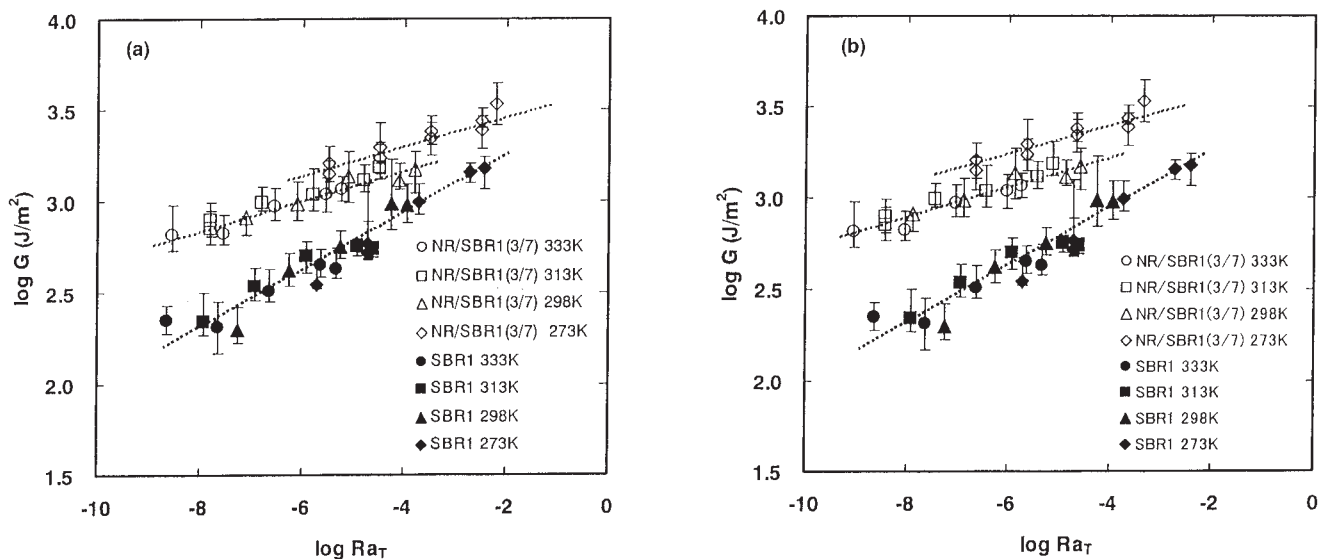
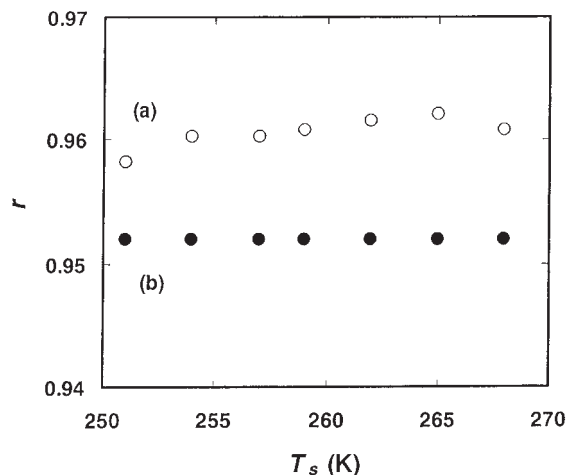


Figure 6 Master curves of  $G$  for the NR/SBR1 blend and SBR1. (a)  $a_T$  of SBR1 was used for both the blend and SBR1, and (b)  $a_T$  of NR was used only for the blend.



**Figure 7** Plot of  $r$  versus  $T_s$  for the NR/SBR1 blend: (a) 298, 313, and 333 K and (b) 273 K.

guished from the deviation of the  $G$  value at 273 K from the master curve for NR/SBR1 and the reinforcing effect of NR on  $G$ . This demonstrates that the strain-induced crystallization of dispersed NR may have played an important role in the enhancement of  $G$ , which depended on the temperature, crosslink density, strain, rate of strain, and so forth.

Furthermore, we investigated the effect of the fatty acid on  $G$ , that is, the strain-induced crystallization. To avoid any difficulty due to the structural change in the NR/SBR1 blend, the blend used in Figure 3 was extracted with acetone, and the removal of the fatty acid was confirmed by infrared spectroscopy, as reported in a previous work.<sup>17</sup> Figure 10 presents a plot of  $G$  for the acetone-extracted NR/SBR1 (NR/SBR1-AE) blend with respect to  $Ra_T$ , for which  $a_T$  for SBR1 was used. A single master curve was drawn, as in the case of the

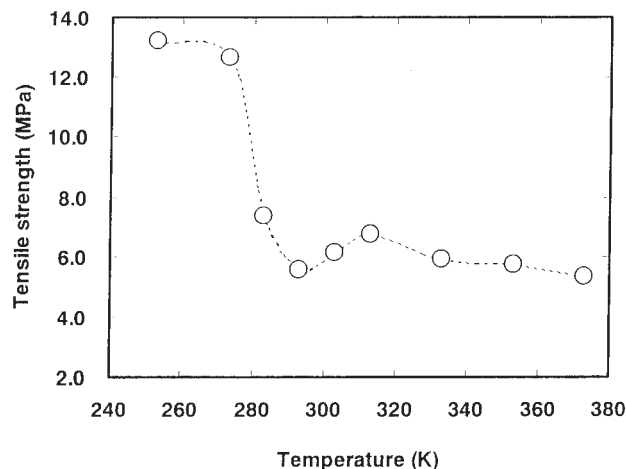


**Figure 8** Temperature dependence of the tensile strength of NR, the crosslink density of which was identical to that of the NR phase in the NR/SBR1 blend.

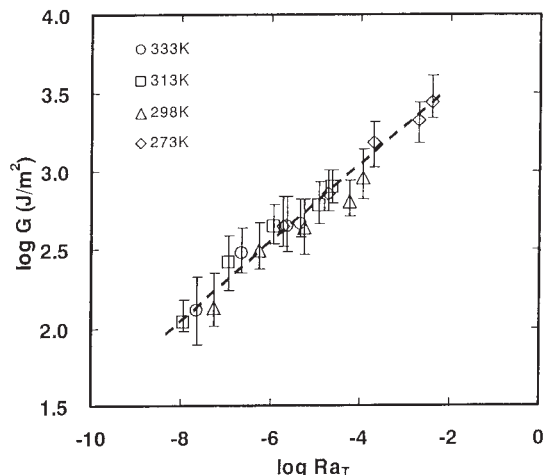


**Figure 9** Master curve of  $G$  for the SBR2/SBR1 blend for which  $a_T$  of SBR1 was used.

SBR2/SBR1 blend. This was quite different from the two curves for  $G$  that appeared for the NR/SBR1 blend after superposition. The difference may be due to the effect of the fatty acid because the fatty acid was mainly removed by acetone extraction, as evident from the previous work.<sup>17</sup> This may suggest that the fatty acid promoted the strain-induced crystallization of NR.

Figure 11 shows the temperature dependence of the tensile strength for acetone-extracted NR (NR-AE), the crosslink density of which was the same as that of the NR domain in NR/SBR1-AE. The tensile strength of NR-AE fell at about 293 K, which was the same as the melting temperature of the strain-induced crystal of NR. This demonstrated that the melting temperature of the strain-induced crystal was not affected by the fatty acid. Because the difference in the master curve

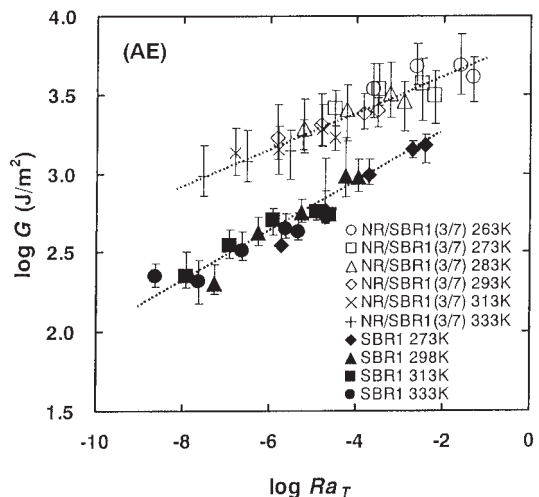


**Figure 10** Master curve of  $G$  for the acetone-extracted strips of the NR/SBR1 blend for which  $a_T$  of SBR1 was used.

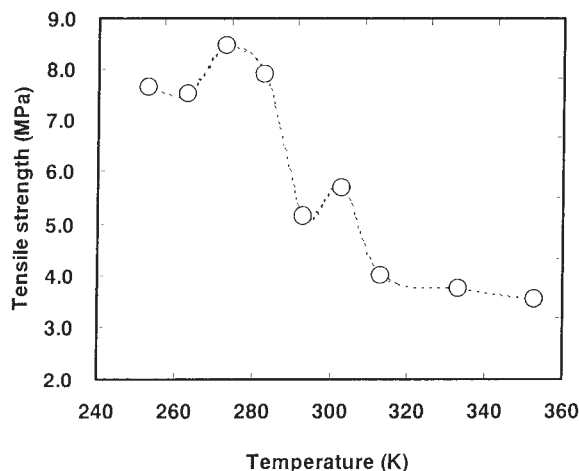


**Figure 11** Temperature dependence of the tensile strength of NR-AE, the crosslink density of which was identical to that of the NR phase in the NR/SBR1-AE blend.

for  $G$  after superposition between the NR/SBR1 and acetone-extracted NR/SBR blends may be anticipated due to the suppression of the strain-induced crystallization after acetone extraction, it is possible to think of the effect of the fatty acid on the strain-induced crystallization, as in the case of the isothermal crystallization of unstrained NR.<sup>4,5</sup>

### CONCLUSIONS

$G$  of SBR1 increased dramatically after SBR1 was mixed with strain-induced crystallizable NR, but not with SBR2, which had a higher 1,2-isomeric unit content. The crosslink density of SBR1 was similar to that of SBR1 in the immiscible NR/SBR1 and SBR2/SBR1 blends.  $G$  of the NR/SBR1 blend at 273 K showed an abrupt increase from about 500 to 1000 J/m<sup>2</sup>, apart

from the curve drawn at higher temperatures ranging from 298 K to 333 K, after the application of the principle of time-temperature superposition. It was different from the results from the superposition of  $G$  for SBR1 and the SBR2/SBR1 blend. For the NR/SBR1 blend after acetone extraction,  $G$  of the blend drew a single curve after the superposition, as in the case of SBR1 and the SBR2/SBR1 blend. This demonstrates that most probable cause of the abrupt increase in  $G$  for the NR/SBR1 blend was the strain-induced crystallization of NR, which was promoted by the effect of the fatty acid.

### References

- Gent, A. N.; Kawahara, S.; Zhao, J. *Rubber Chem Technol* 1998, 71, 668.
- Kawazura, T.; Kawahara, S.; Isono, Y. *Rubber Chem Technol* 2003, 76, 1164.
- Kawazura, T.; Kawahara, S.; Isono, Y., submitted.
- Tanaka, Y.; Kawahara, S.; Tangpakdee, J. *Kautsch Gummi Kunstst* 1997, 50, 6.
- Kawahara, S.; Kakubo, T.; Sakdapipanich, J. T.; Isono, Y.; Tanaka, Y. *Polymer* 2000, 41, 7483.
- Ferry, J. D. *Viscoelastic Properties of Polymers*; Wiley: New York, 1961; Chapter 11.
- Wang, Y. F.; Wang, C. *Rubber Chem Technol* 1997, 70, 663.
- Flory, P. J.; Rehner, J. *J Chem Phys* 1943, 11, 521.
- Bristow, G. M.; Watson, W. F. *Trans Faraday Soc* 1958, 54, 1731.
- Tewari, Y. B.; Schreiber, H. P. *Macromolecules* 1972, 5, 329.
- Thomas, A. G.; Whittle, J. M. *Rubber Chem Technol* 1970, 43, 222.
- Stager, R. G.; von Meerwall, E. D.; Kelley, F. N. *Rubber Chem Technol* 1985, 58, 913.
- Gent, A. N.; Lai, S. M.; Nah, C.; Wang, C. *Rubber Chem Technol* 1994, 67, 610.
- Gent, A. N.; Lai, S. M. *J Polym Sci Part B: Polym Phys* 1994, 32, 1543.
- Smith, T. L. *Polym Eng Sci* 1965, 5, 270.
- Greensmith, H. W.; Thomas, A. G. *J Polym Sci* 1955, 18, 189.
- Tanaka, Y. *Rubber Chem Technol* 2001, 74, 355.